

UNCLASSIFIED

SECURITY CLASSIFICATION OF THIS PAGE (When Data Entered)

AD-A087929

REPORT DOCUMENTATION PAGE

READ INSTRUCTIONS BEFORE COMPLETING FORM

1. REPORT NUMBER NSWC/TR-80-204	2. GOVT ACCESSION NO. AD-A087929	3. RECIPIENT'S CATALOG NUMBER 929
4. TITLE (and Subtitle) DETERMINATION OF KINETIC PARAMETERS FOR THERMAL DECOMPOSITION OF PHENOLIC ABLATIVE MATERIALS BY MULTIPLE HEATING RATE METHOD.		5. TYPE OF REPORT & PERIOD COVERED Final Repts
7. AUTHOR(s) J. B. Henderson M. R. Tant J. A. Wiebelt G. R. Moore		8. CONTRACT OR GRANT NUMBER(s) 11 Jul 80
9. PERFORMING ORGANIZATION NAME AND ADDRESS Naval Surface Weapons Center (N43) Dahlgren, VA 22448		10. PROGRAM ELEMENT, PROJECT, TASK AREA & WORK UNIT NUMBERS OPN 12 337
11. CONTROLLING OFFICE NAME AND ADDRESS Naval Sea Systems Command Washington, DC 20362		12. REPORT DATE July 1980
14. MONITORING AGENCY NAME & ADDRESS (if different from Controlling Office) 16 ZR00001 17 ZR0000101		13. NUMBER OF PAGES 34
		15. SECURITY CLASS. (of this report) UNCLASSIFIED
		15a. DECLASSIFICATION/DOWNGRADING SCHEDULE

16. DISTRIBUTION STATEMENT (of this Report)
Approved for public release; distribution unlimited.

17. DISTRIBUTION STATEMENT (of the abstract entered in Block 20, if different from Report)
Agreed

18. SUPPLEMENTARY NOTES

19. KEY WORDS (Continue on reverse side if necessary and identify by block number)
ablation activation energy
phenolic ablative materials reaction order
kinetic rate equation pre-exponential factor
kinetic parameters

20. ABSTRACT (Continue on reverse side if necessary and identify by block number)
The rate of decomposition for two widely used glass- and asbestos-phenolic ablative materials were measured using standard thermogravimetric techniques. Thermograms were obtained at six heating rates ranging from 10°C/min to 160°C/min. From these data, the kinetic parameters were determined by a slightly modified version of Friedman's method. Fractional weight loss calculated using the derived kinetic parameters over the temperature range of decomposition agreed with measured values with a mean error of 0.33 and

skk

UNCLASSIFIED

SECURITY CLASSIFICATION OF THIS PAGE (When Data Entered)

20. ABSTRACT (Continued)

0.28 percent, with a standard deviation of errors 0.58 and 0.84 percent for glass- and asbestos-phenolic, respectively. The 95-percent confidence for the mean error was 0.22 and 0.44 percent for the glass-phenolic and 0.14 and 0.42 percent for the asbestos-phenolic. Also, the activation energy was calculated by the Flynn and Wall method. The average activation energy values determined by the two methods agreed within 4.6 percent for both materials.



UNCLASSIFIED

SECURITY CLASSIFICATION OF THIS PAGE (When Data Entered)

FOREWORD

This work was performed as part of an investigation to screen and classify candidate ablative materials for use in shipboard applications. Funds were provided by Naval Sea Systems Command (SEA-62R) and by NSWC independent research program Task Area Number ZR000-01-01.

This work was reviewed and approved by J. J. Yagla, Head, Ship Safety Engineering Branch, and J. F. Horton, Head, Systems Safety Division.

Released by:

A handwritten signature in black ink, appearing to read "G. O. Miller". The signature is written in a cursive style with a vertical line through the middle of the name.

G. O. MILLER, Head
Combat Systems Department

CONTENTS

	<u>Page</u>
INTRODUCTION	1
BACKGROUND	1
THEORY	2
FRIEDMAN'S METHOD	2
DISCUSSION OF FRIEDMAN TECHNIQUE.....	3
FLYNN AND WALL METHOD	3
EXPERIMENTAL.....	4
MATERIALS	4
APPARATUS AND PROCEDURE	5
RESULTS	5
DISCUSSION	21
REFERENCES	21
DISTRIBUTION	

Accession For	
RTIG GRA&I	<input checked="" type="checkbox"/>
DDC TAB	<input type="checkbox"/>
Unannounced Justification	
By _____	
Distribution/	
Availability Codes	
Dist	Avail and/or special
A	

INTRODUCTION

The rate of decomposition of an ablative material when heated is modeled by the kinetic rate equation. If it is assumed that the material dimensions are constant, the rate equation determines the density of the remaining char. Both the rate of decomposition and char density strongly affect the thermal performance of the material. In order to predict the thermal response, accurate values of the kinetic parameters over the entire range of decomposition are required. In the case of an ablative material exposed to a solid rocket motor exhaust, the heat flux may vary widely depending upon the geometry and/or type of motor. Therefore, the effect of the heating rate on the kinetic parameters must be known as well.

The purpose of this study was to determine an appropriate model for the rate of decomposition of ablative materials. Friedman's method¹ using multiple heating rates was chosen, since ablative materials are subjected to widely varying heating rates. Application of this method required calculating an average activation energy for the entire thermal decomposition. The decomposition reaction required two models, one for the initial decomposition and another for the remainder. For these two regions, separate pre-exponential factors and apparent orders of reaction were calculated by the technique developed by Friedman.¹ For comparison, the average activation energy for each material determined by Friedman's method was compared to the value obtained by the method of Flynn and Wall.²

BACKGROUND

The decomposition kinetics of solid materials have been studied by many investigators. As a result, numerous techniques have been developed to extract the kinetic parameters from experimental data.

Freeman and Carroll³ developed the well-known difference method and applied the technique to determine the kinetic parameters for calcium oxalate monohydrate. The method was later revised by Anderson and Freeman⁴ and applied to the study of polystyrene and polyethylene. Mickelson and Einhorn⁵ developed the ratio method to analyze thermogravimetric data obtained for a urethane polymer. Baer, Hedges, Seader, Jayakar, and Wojcik⁶ heated samples of reinforced polymers at heating rates up to 4200°C/min. The data were correlated by a numerical technique developed by Burningham and Seader.⁷ Friedman¹ studied the decomposition of a fiberglass-phenolic based on a technique developed for multiple heating rates. Similarly, Flynn and Wall² developed a method for determining the activation energy based on data taken at several different heating rates.

Baer, *et al.*⁶ discussed the fact that kinetic parameters obtained by methods using a single thermogram at low heating rates do not accurately predict kinetic behavior when applied to the higher heating rates. For this reason, the methods of Friedman¹ and Flynn and Wall² were considered in this work.

THEORY

FRIEDMAN'S METHOD

Friedman's method is attractive for this application because the kinetic properties may be calculated based on data taken over a wide range of heating rates. Further, the Arrhenius equation is combined with an arbitrary function of weight. This allows more flexibility, since no prior knowledge of the function is required. This method does, however, require measurement of the weight loss and rate of weight loss as a function of temperature at several different heating rates.

The general form of the rate equation proposed by Friedman is

$$-1/W_0 \times dW/dt = Af(W/W_0) \exp(-E/RT) \quad (1)$$

where

W_0	=	original weight of material (mg)
dW/dt	=	rate of weight loss (mg/min)
A	=	pre-exponential factor (min^{-1})
E	=	activation energy (cal/gm-mole)
R	=	gas constant (1.987 cal/gm-mole-°K)
T	=	temperature (°K)
$f(W/W_0)$	=	undefined function of weight

Taking the natural logarithm of both sides of Equation (1) results in

$$\ln[-1/W_0 \times dW/dt] = \ln[Af(W/W_0)] - E/RT \quad (2)$$

A linear equation may be fit to $\ln[-1/W_0 \times dW/dt]$ as a function of $1/T$ at constant parametric values of W/W_0 . These equations will have slopes of $-E/R$. Each intercept is the value of $\ln[Af(W/W_0)]$ at the parametric value of W/W_0 . Then, by defining

$$f(W/W_0) = [(W - W_f)/W_0]^n \quad (3)$$

where

n	=	order of reaction
W	=	instantaneous weight of material (mg)
W_f	=	final weight of charred material (mg)

and multiplying Equation (3) by A and taking the natural logarithm results in

$$\ln[Af(W/W_0)] = \ln A + n \ln[(W - W_f)/W_0] \quad (4)$$

The final ratio, W_f/W_o , is taken from the original thermograms. Since $\ln[Af(W/W_o)]$ is known for various W/W_o ratios, Equation (4) can be used to obtain values of A and n.

DISCUSSION OF FRIEDMAN TECHNIQUE

Friedman used this technique to calculate the kinetic properties for CTL91-LD fiberglass-phenolic. One activation energy was calculated for each of the 12 values of weight loss ranging from 0.675 to 0.95 (on a glass-free basis). The average activation energy was calculated from these data. By eliminating the early weight loss ($\approx 4\%$) and dropping the data points above $W/W_o = 0.875$ and using $W_f/W_o = 0.61$, a linear curve was fit to the data. Thus, the effective range covered by the curve fit was approximately $0.65 \leq W/W_o \leq 0.85$, which accounted for about 50 percent of the total weight loss. This resulted in a rather poor fit of the data at both ends of the weight loss curve. In contrast, the requirement for the present application was to obtain a kinetic expression applicable over the entire range of weight loss.

Three points regarding this method should be clarified. First, the equation of $f(W/W_o)$ may take a variety of forms. For example, Goldfarb, McGuchan and Meeks⁸ selected $f(W/W_o) = [(W - W_f)/W_o - W_f/W_o]^n$: This will result only in a change in the intercept $\ln A$; i.e., a change in the apparent pre-exponential factor.

Secondly, the kinetic parameters may be calculated by considering either the total weight or only the resin weight of the sample. Again the activation energy and order of reaction remain unchanged. Only the intercept $\ln A$ is affected.

Using a pre-exponential factor based only on the resin weight will result in an error, if used in calculations where the total weight is being considered. Assuming the unknown function is $[(W - W_f)/W_o]^n$, the two pre-exponential factors are related by:

$$A' = A[(W_o - W_g)/W_o]^{n-1} \quad (5)$$

where

$$\begin{aligned} A' &= \text{pre-exponential factor (resin weight only)}(\text{min}^{-1}) \\ W_g &= \text{weight of inert material (mg)} \end{aligned}$$

Finally, changes in the activation energy at different degrees of conversion may be a result of real changes due to a change in mechanism, to a change in structure of the resin, or to a result of experimental error. If these changes are not a result of experimental error, then using $E = E(W/W_o)$ would be more realistic. In many cases, however, separation of the experimental error from real changes in E is difficult.

FLYNN AND WALL METHOD

Flynn and Wall² developed a convenient method to determine the activation energy from weight loss curves measured at several heating rates. The following relationship is used to calculate the activation energy.

$$E \approx - (R/C) d \log \beta / d(1/T) \quad (6)$$

where

$$\beta = \text{heating rate } (^{\circ}\text{C}/\text{min})$$

$$C = C(E/RT)$$

Plotting $1/T$ versus $\log \beta$ at several weight loss ratios results in a series of straight lines with slope $\Delta \log \beta / \Delta (1/T)$. Using the slope and the appropriate value of C , the activation energy can be calculated by Equation (6). Since C is a function of E/RT , the calculation of E from Equation (6) is an iterative process. Flynn and Wall constructed a table of values for C over the range from $7 \leq E/RT \leq 60$. The variation of C over this range is approximately ± 3 percent. This method is extremely attractive, since it involves only reading the temperature at a constant weight loss from a series of thermograms at different heating rates.

EXPERIMENTAL

MATERIALS

The two ablative materials studied were supplied by Havg Industries. As shown in Table 1, these materials consisted of a phenol-formaldehyde resin with specified amounts of glass, asbestos, and/or magnesium silicate added as filler.

The materials were converted to powder form by machining and were then filtered through a No. 20 sieve. They were stored overnight in a vacuum dessicator maintained at 35°C to remove traces of water.

Table 1. Composition of Material Tested

Contents	Material Composition	
	H41NE (%)	H41D (%)
Asbestos	—	52.0
Glass (SiO_2) and Magnesium Silicate	60.5	—
Total Filler Content	60.5	52.0
Phenol-Formaldehyde Resin (H41P)	39.5	48.0
Total Nonvolatiles	60.5	52.0

APPARATUS AND PROCEDURE

A Perkin-Elmer TGS-2 Thermogravimetric System was used, with temperature control provided by a Perkin-Elmer System 4 Microprocessor Controller. The sample temperature was measured with a chromel-alumel thermocouple, which was calibrated with a set of five Curie standards in the temperature range of interest at each heating rate used.⁹

In order to reduce temperature gradients in the material and to ensure uniform heating, small weights of a powdered form of the materials were used. Samples weighing 7.5 ± 0.5 mg were heated from 40 to 950°C using heating rates of 10, 20, 40, 80, 100, and 160°C/min. Both the percentage of initial weight and the rate of weight loss were plotted directly as a function of temperature. The samples were maintained in a nitrogen atmosphere throughout the experiment. When the programmed temperature scan reached 950°C, the purge gas was automatically switched to oxygen to thermo-oxidatively degrade the remaining resin. To verify the initial weight fraction of filler, the temperature was held at 950°C until the resin had completely degraded.

RESULTS

The original thermograms contained the temperature, derivative of weight loss, and the fraction of weight remaining. These data were digitized at 0.01 intervals of the fraction of weight remaining. The experimental temperatures were corrected using the Curie standard temperature calibration for each heating rate. The thermograms were then reproduced from this data. Figures 1 through 6 and 7 through 12 show the fraction of weight remaining and the rate of weight loss as a function of temperature and time for each heating rate for H41NE and H41D, respectively. Comparisons of the fraction of weight remaining as a function of temperature at all six heating rates for H41NE and H41D are shown in Figures 13 and 14. Figures 15 and 16 depict the relative magnitudes of the derivative of weight loss as a function of temperature at all six heating rates for H41NE and H41D, respectively. The digitized data for both materials are listed in the appendix.

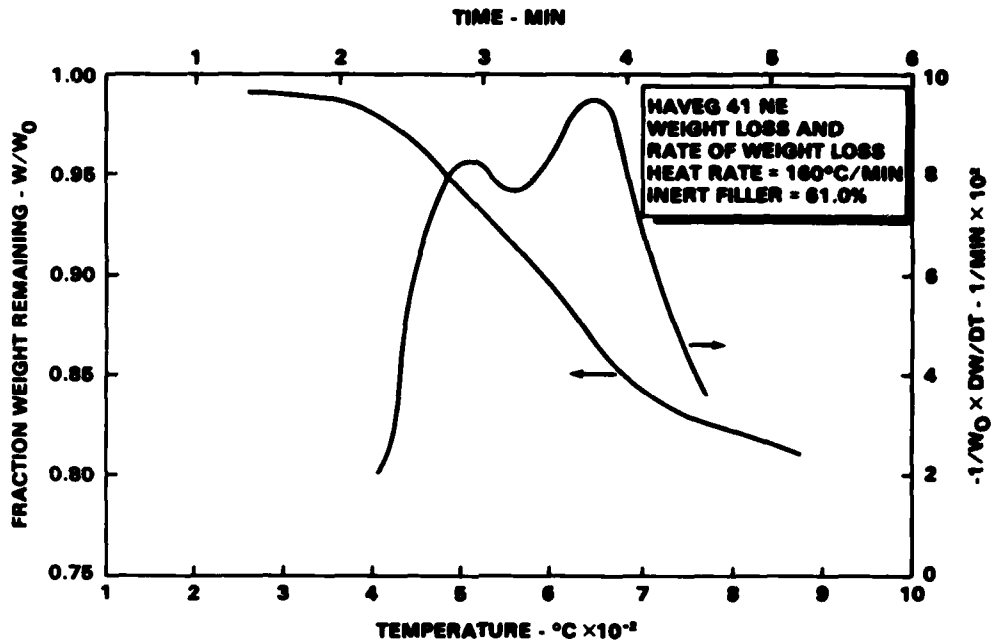


Figure 1. 160°C/min Thermogram for H41NE

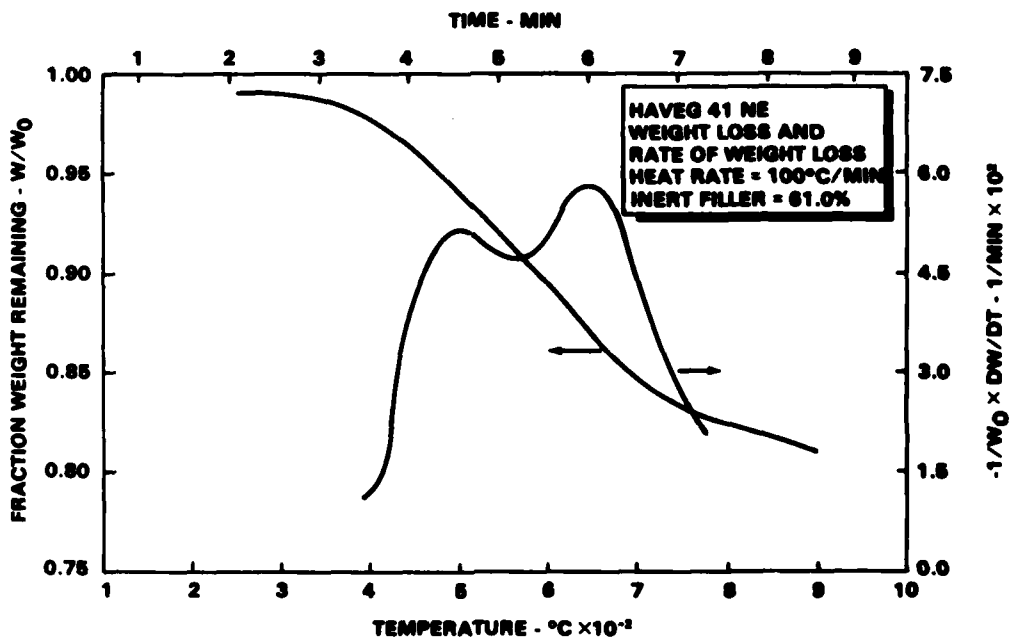


Figure 2. 100°C/min Thermogram for H41NE

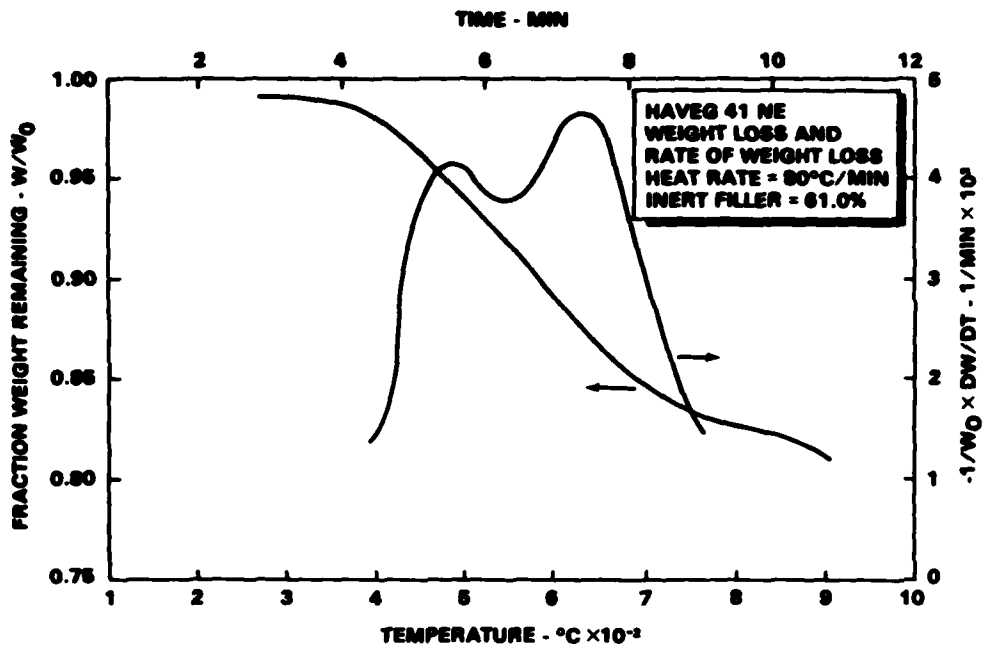


Figure 3. 80°C/min Thermogram for H41NE

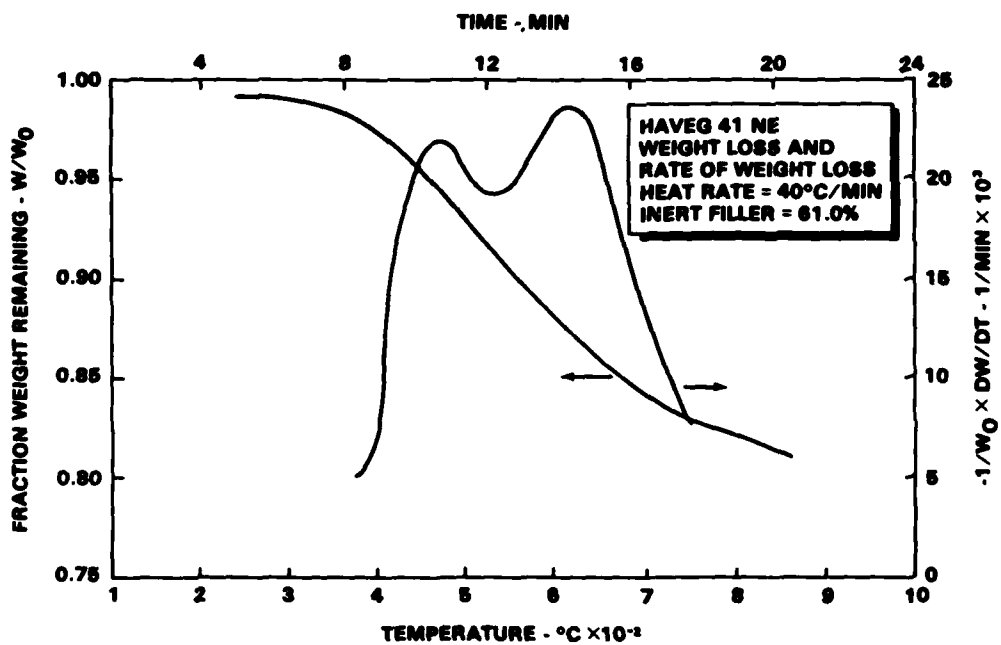


Figure 4. 40°C/min Thermogram for H41NE

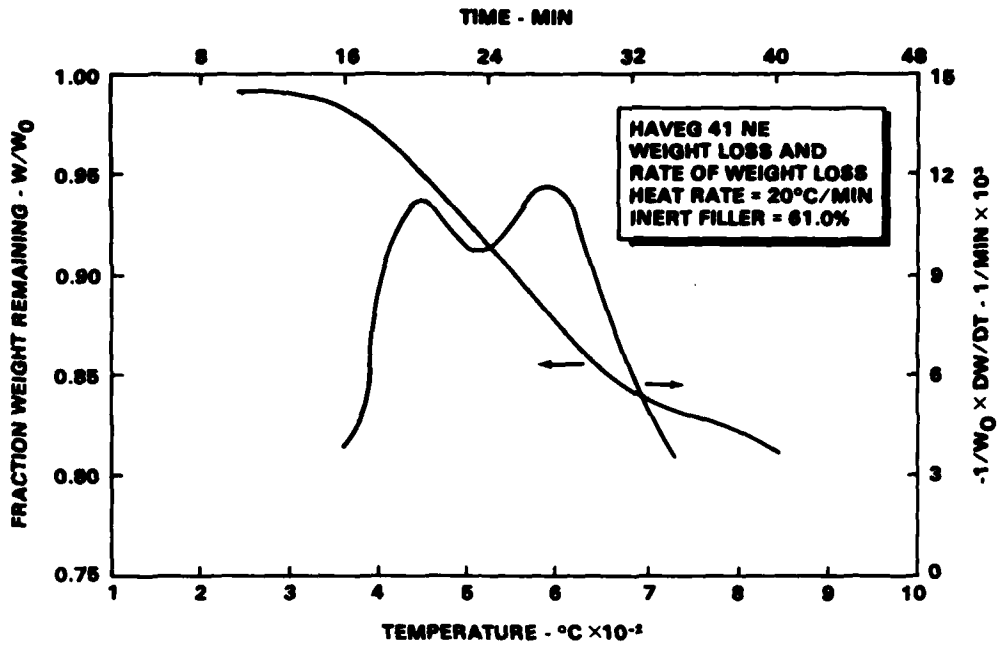


Figure 5. 20°C/min Thermogram for H41NE

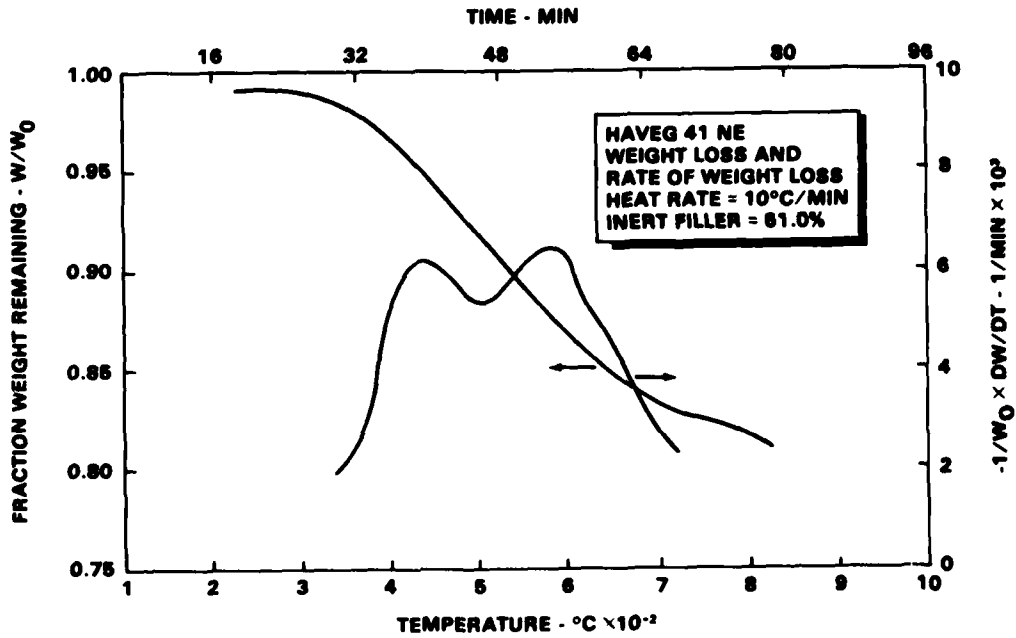


Figure 6. 10°C/min Thermogram for H41NE

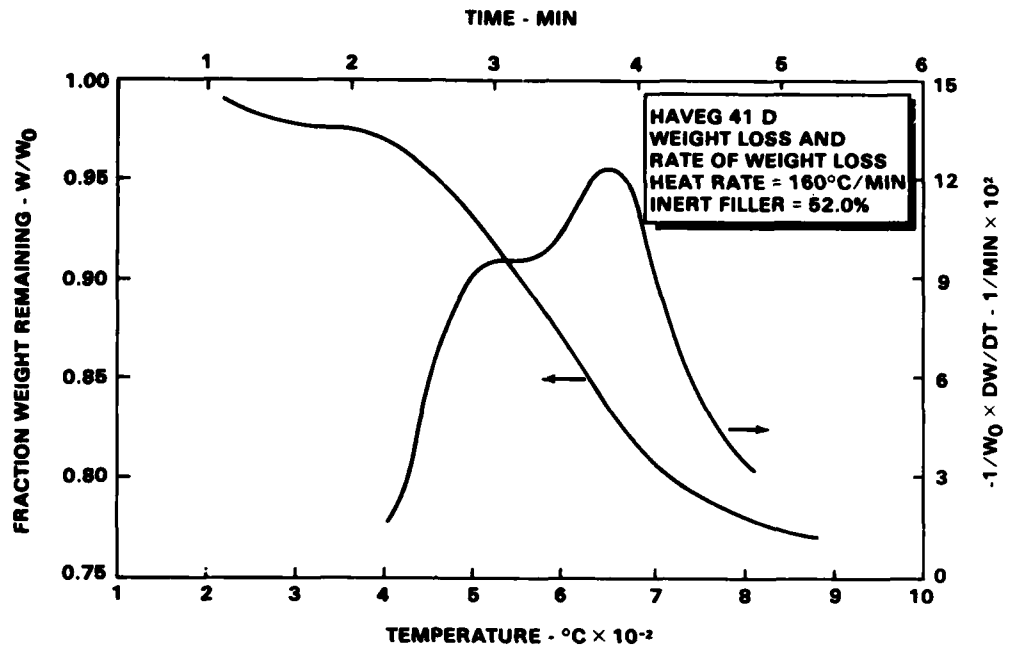


Figure 7. 160°C/min Thermogram for H41D

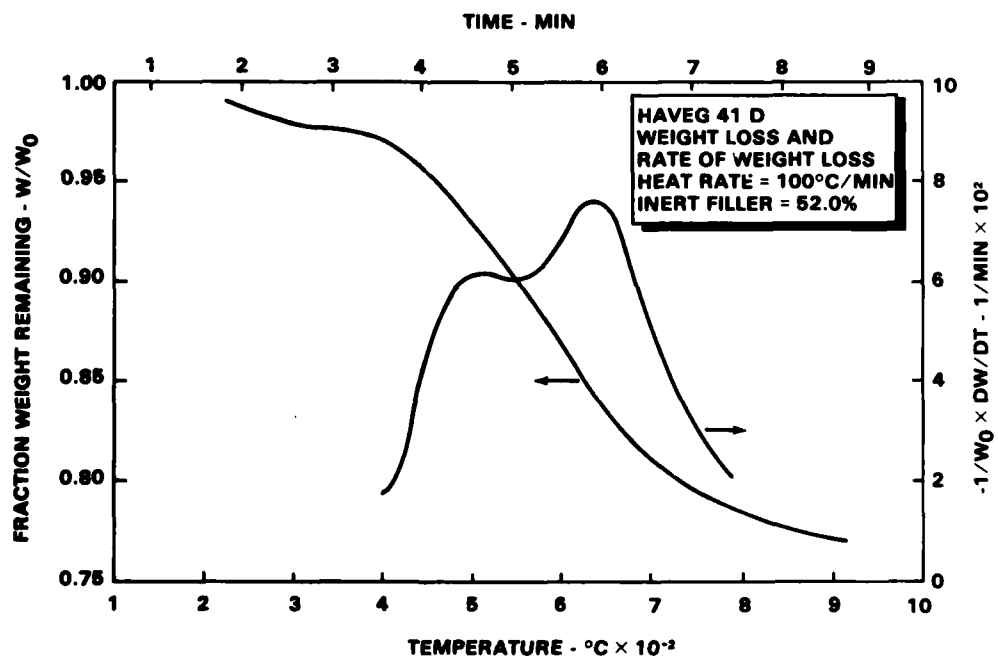


Figure 8. 100°C/min Thermogram for H41D

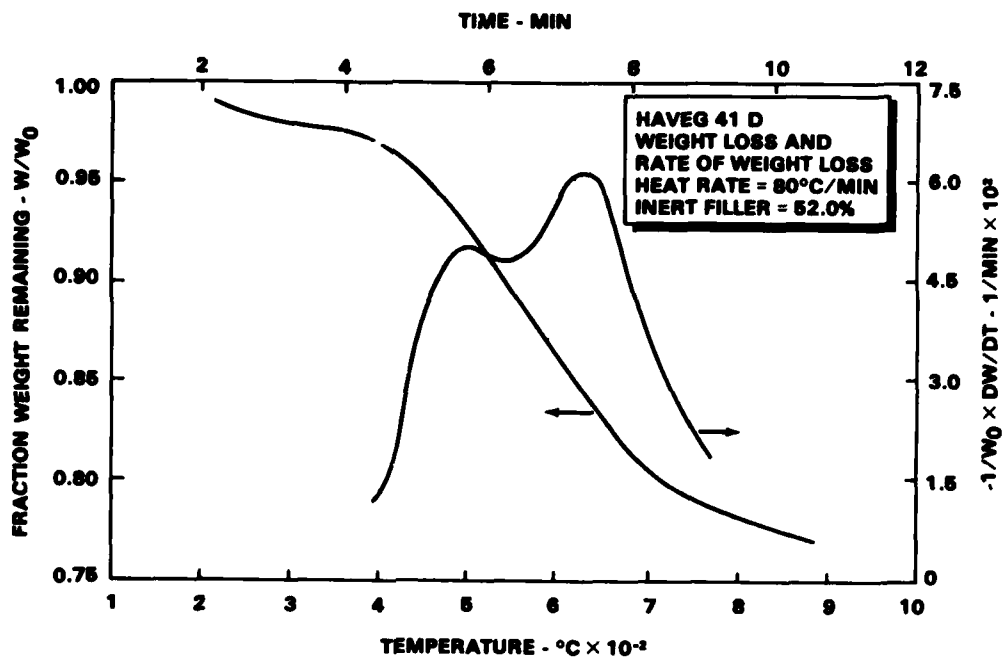


Figure 9. 80°C/min Thermogram for H41D

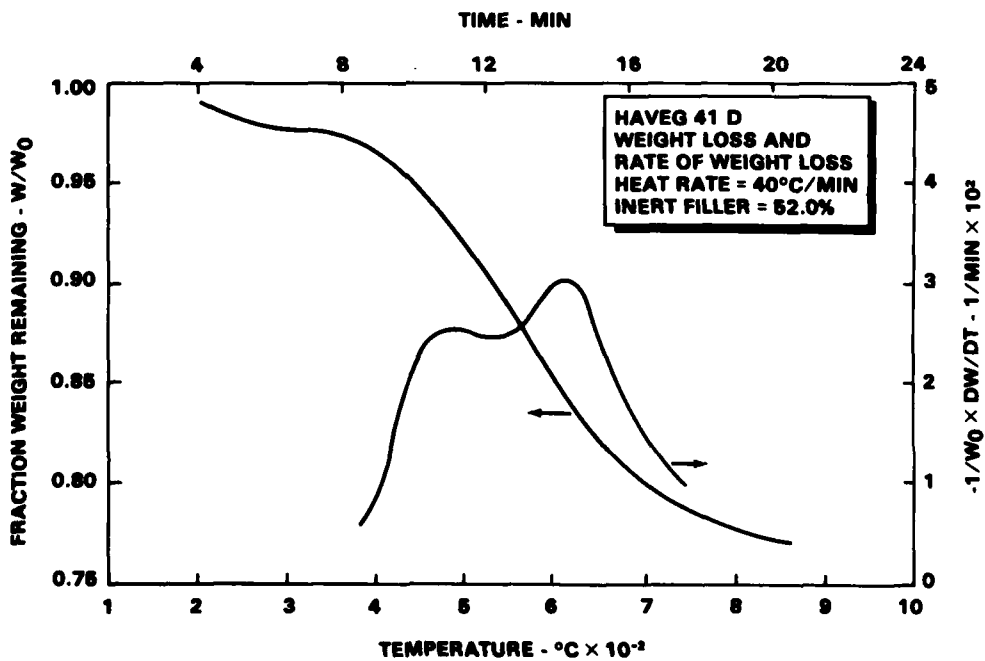


Figure 10. 40°C/min Thermogram for H41D

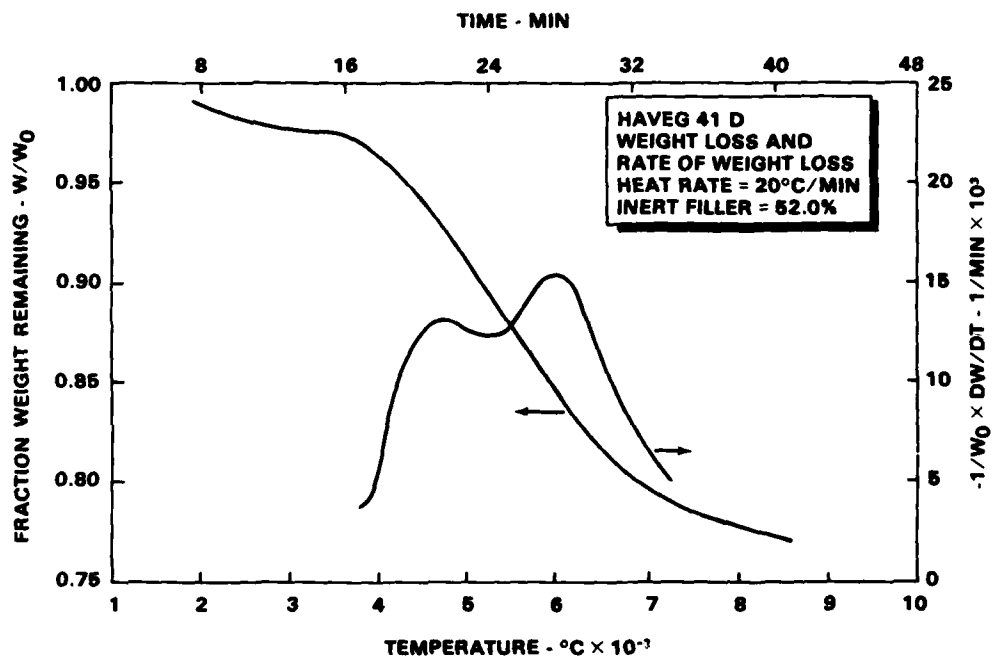


Figure 11. 20°C/min Thermogram for H41D

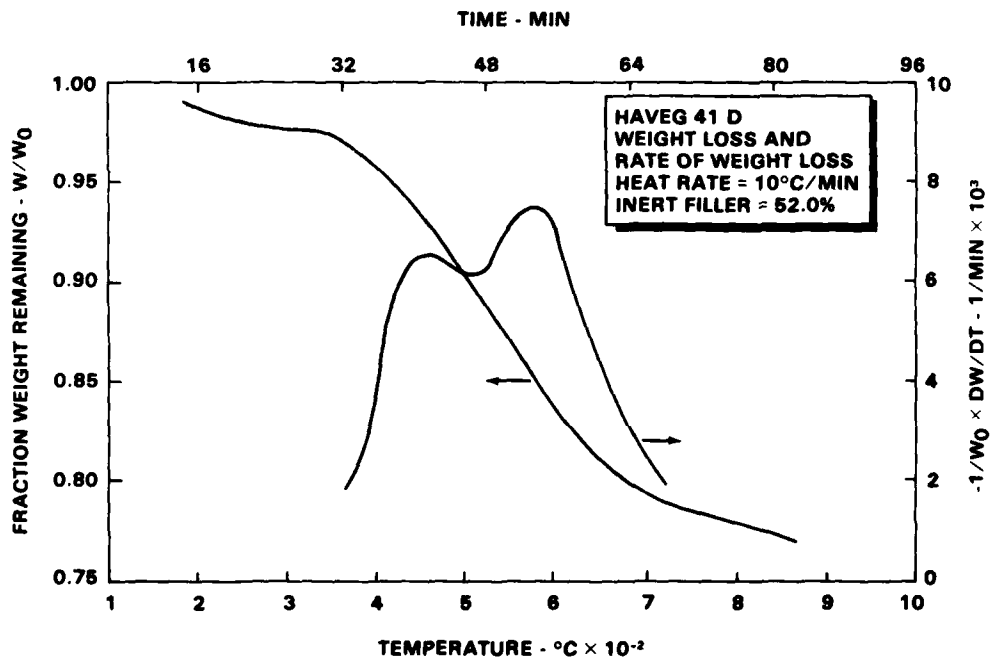


Figure 12. 10°C/min Thermogram for H41D

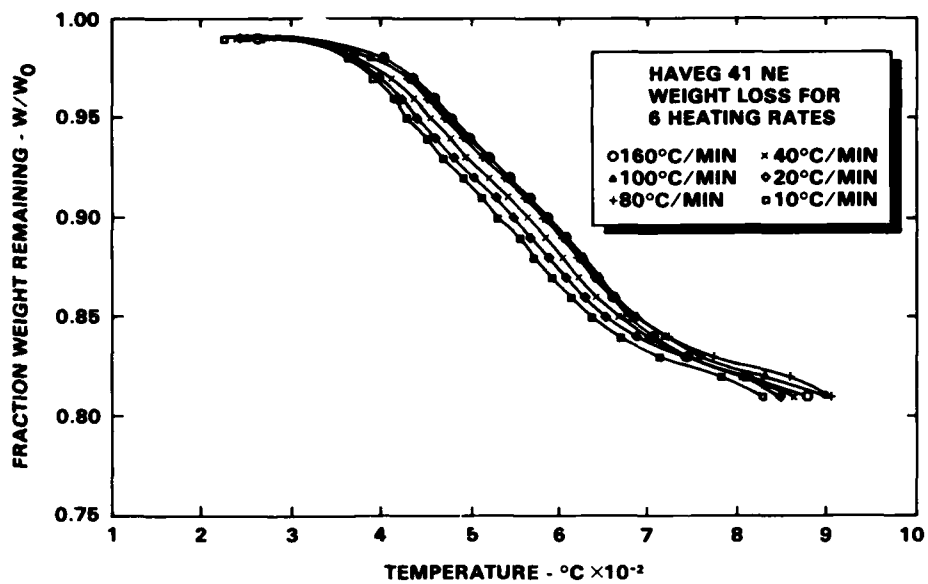


Figure 13. Fraction Weight Remaining for All Six Heating Rates for H41NE

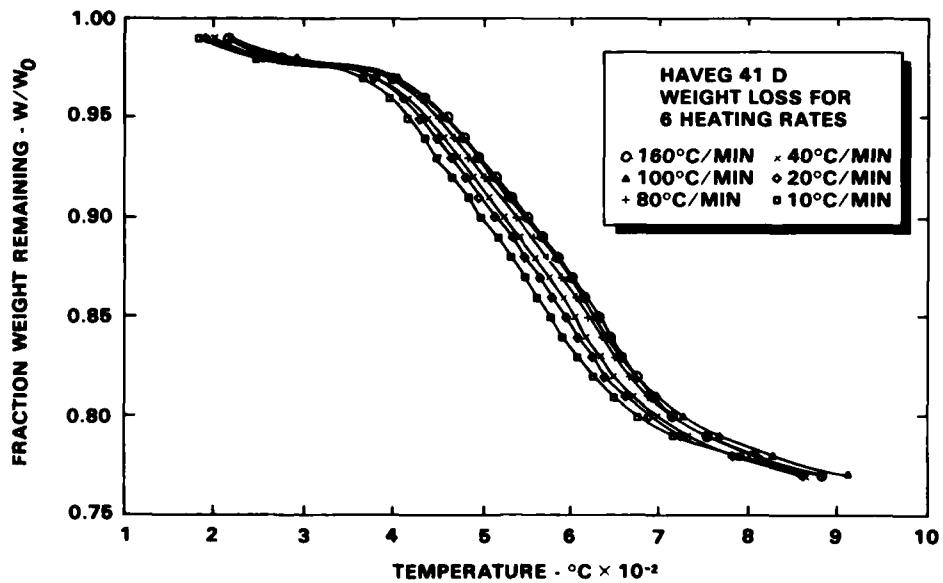


Figure 14. Fraction Weight Remaining for All Six Heating Rates for H41D

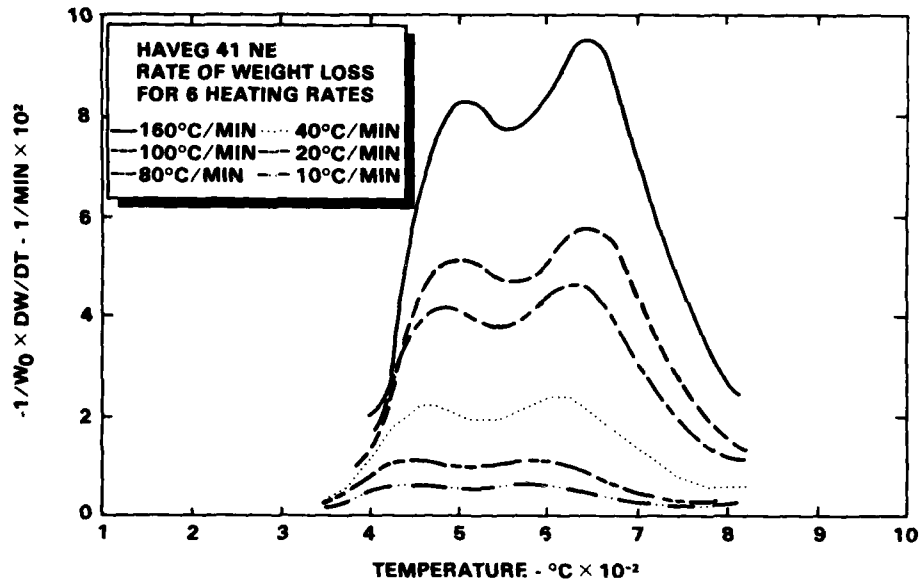


Figure 15. Derivatives of Weight Loss for All Six Heating Rates for H41NE

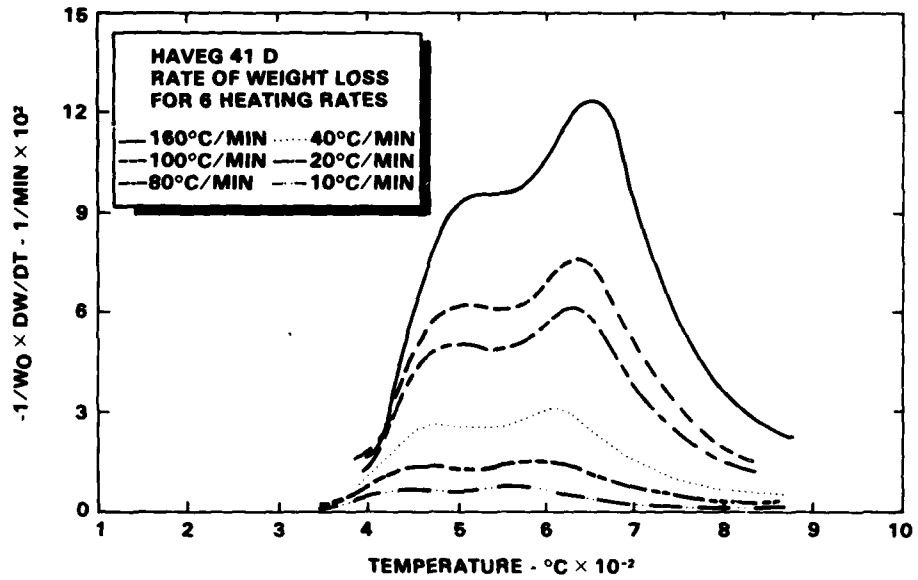


Figure 16. Derivatives of Weight Loss for All Six Heating Rates for H41D

A plot of $\ln[-1/W_0 \times dW/dt]$ versus $1/T$ for H41NE is shown in Figure 17. Figure 18 is a single plot for H41D. The slope of each line was determined from a least-squares fit of the data. Figure 19 shows the corresponding activation energy and intercept $\ln[Af(W/W_0)]$ at each value of weight loss from $0.84 < W/W_0 < 0.98$ for H41NE. Figure 20 depicts the same information for H41D over the range from $0.79 < W/W_0 < 0.97$. The range of each data point is the range of error based on the least-squares fit of the data. Values of $\ln[Af(W/W_0)]$ versus $\ln[(W - W_f)/W_0]$ for H41NE are shown in Figure 21 and for H41D in Figure 22. These figures depict the separation of the reaction into the two regions and the corresponding least-squares fit over each region. A pre-exponential factor and order of reaction were determined for each of these two regions. The average activation energies determined from Figures 17 and 18 were used for both regions. Using Flynn and Wall's method, the average activation energies for both materials were calculated based on plots of $\log \beta$ versus $1/T$. The results are shown in Figures 23 and 24 for H41NE and H41D, respectively. A summary of the results of the calculations for both materials is listed in Table 2.

The kinetic parameters calculated by the modified version of Friedman's method were used in Equation (1) to calculate the fraction of weight remaining versus temperature. Each set of parameters was applied to that portion of the weight loss curve from which it was determined. A comparison of the results of these calculations and the experimental data for $10^\circ\text{C}/\text{min}$ and $160^\circ\text{C}/\text{min}$ heating rates for H41NE and H41D are shown in Figures 25 and 26, respectively. The average error, standard deviation of errors and the 95-percent confidence interval were calculated for 90 and 114 experimental versus calculated points for H41NE and H41D, respectively. These results are presented in Table 3.

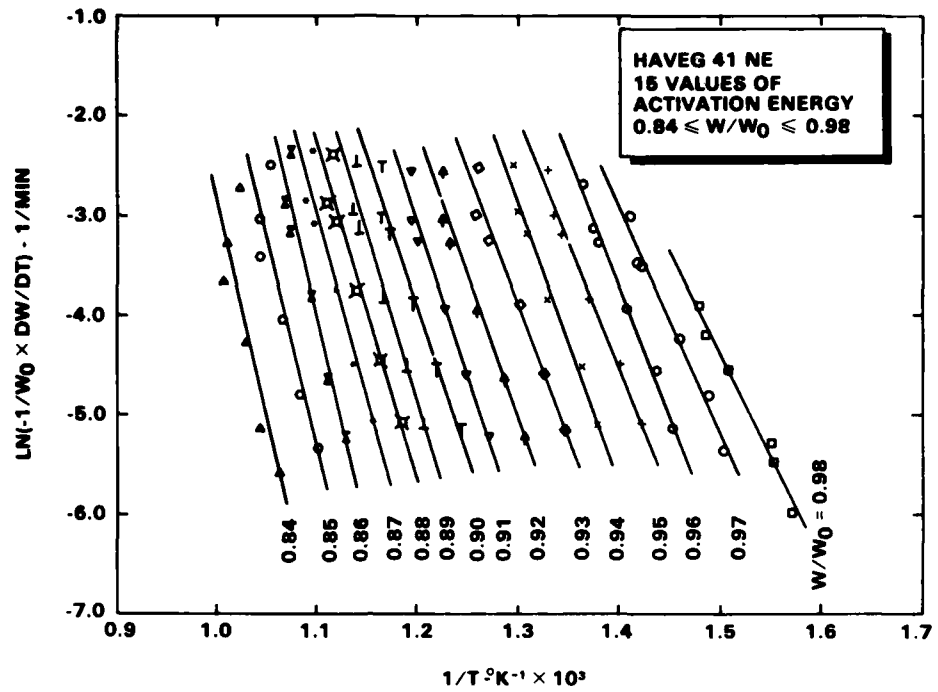


Figure 17. Plot of Slopes Used to Determine the Activation Energy for H41NE

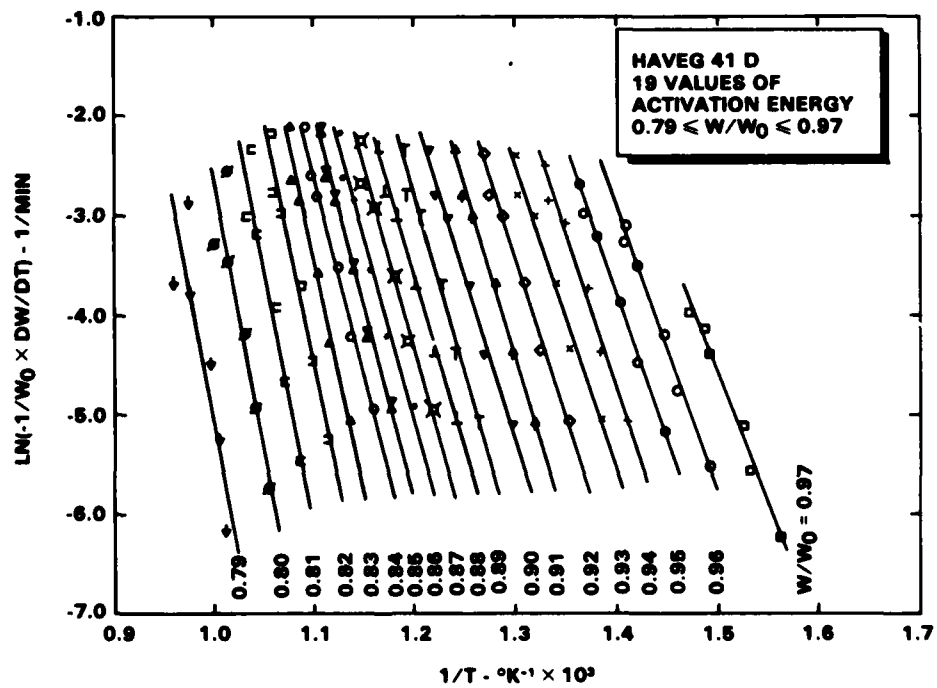


Figure 18. Plot of Slopes Used to Determine the Activation Energy for H41D

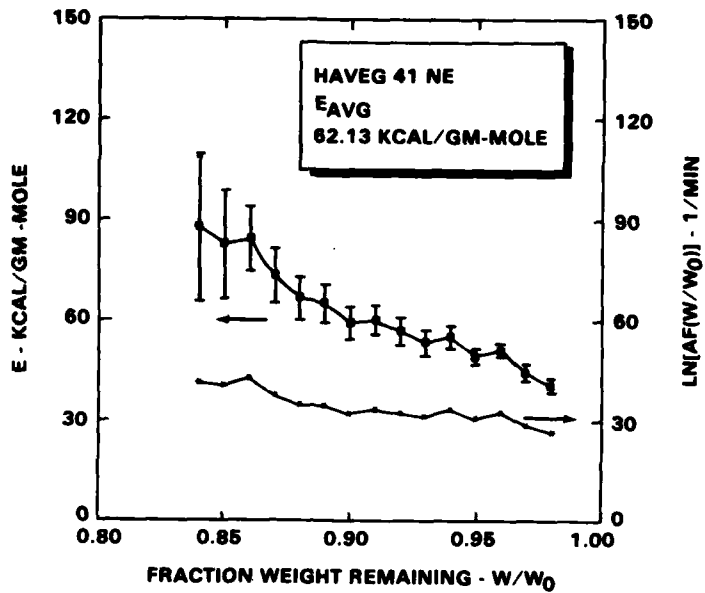


Figure 19. Activation Energy and Intercept as a Function of Degree of Conversion for H41NE

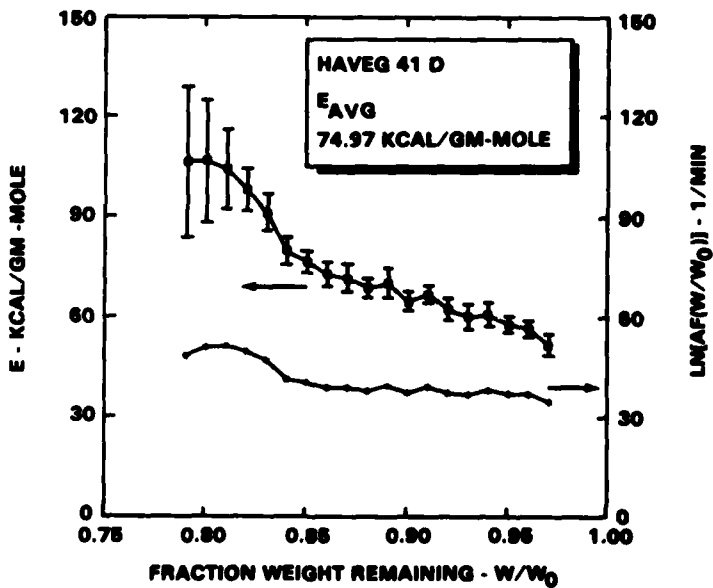


Figure 20. Activation Energy and Intercept as a Function of Degree of Conversion for H41D

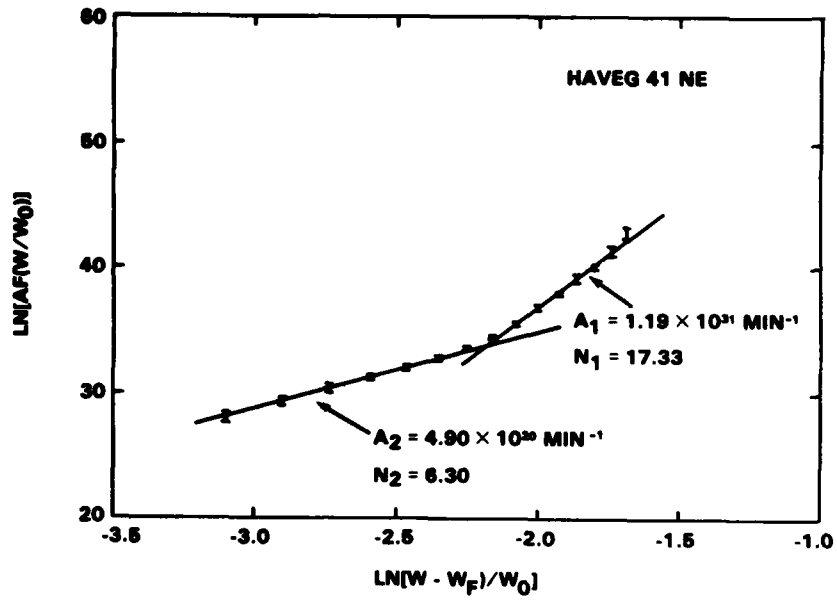


Figure 21. Plot to Determine the Pre-exponential Factor and Order of Reaction for Two Regions of Weight Loss for H41NE

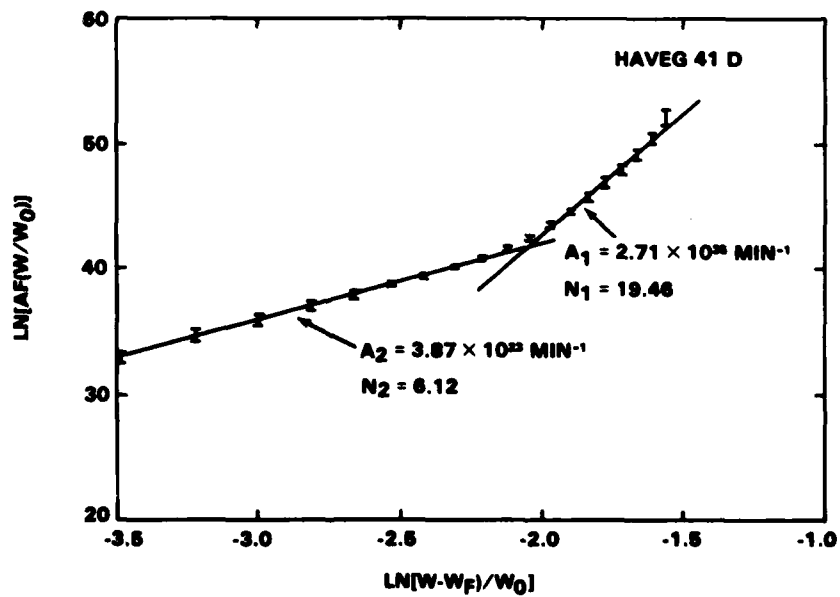


Figure 22. Plot to Determine the Pre-exponential Factor and Order of Reaction for Two Regions of Weight Loss for H41D

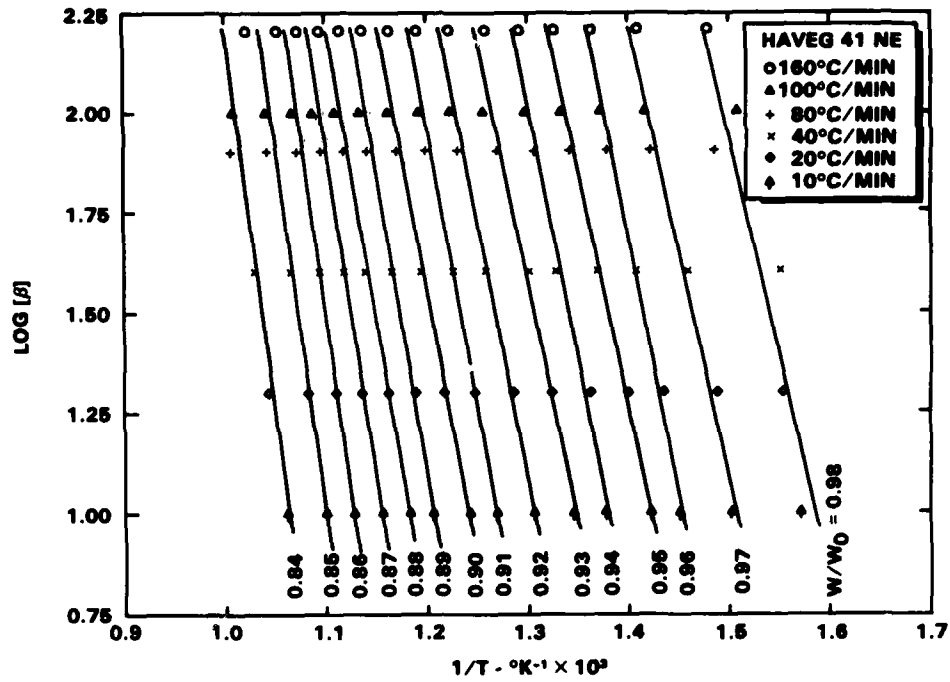


Figure 23. Plot of Slopes Used to Determine the Activation Energy for H41NE by the Method of Flynn and Wall

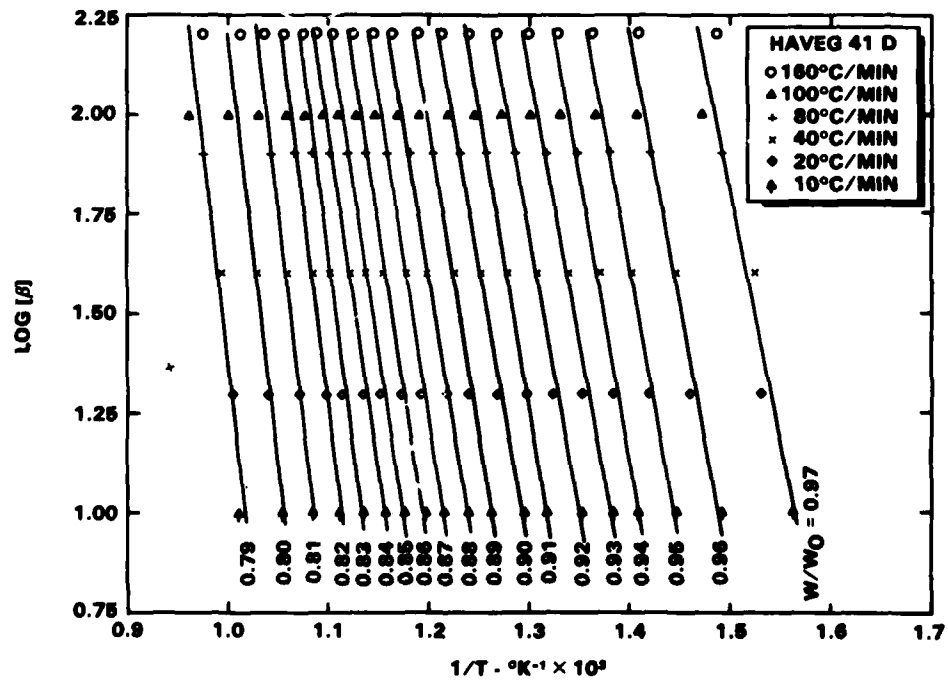


Figure 24. Plot of Slopes Used to Determine the Activation Energy for H41D by the Method of Flynn and Wall

Table 2. Summary of Calculations

<u>Material</u>	<u>W_f/W_o</u>	Range of <u>W/W_o</u>	<u>E_{avg} (kcal/gm-mole)</u>		<u>A (min⁻¹)</u>	<u>n</u>	<u>W/W_o</u>
			<u>Friedman</u>	<u>Flynn & Wall</u>			
H41NE	0.795	0.98 - 0.84	62.13	62.15	1.19 x 10 ³¹	17.33	≥ 0.91
					4.90 x 10 ²⁰	6.30	< 0.91
H41D	0.760	0.97 - 0.79	74.97	71.52	2.71 x 10 ³⁵	19.46	≥ 0.89
					3.87 x 10 ²³	6.12	< 0.89

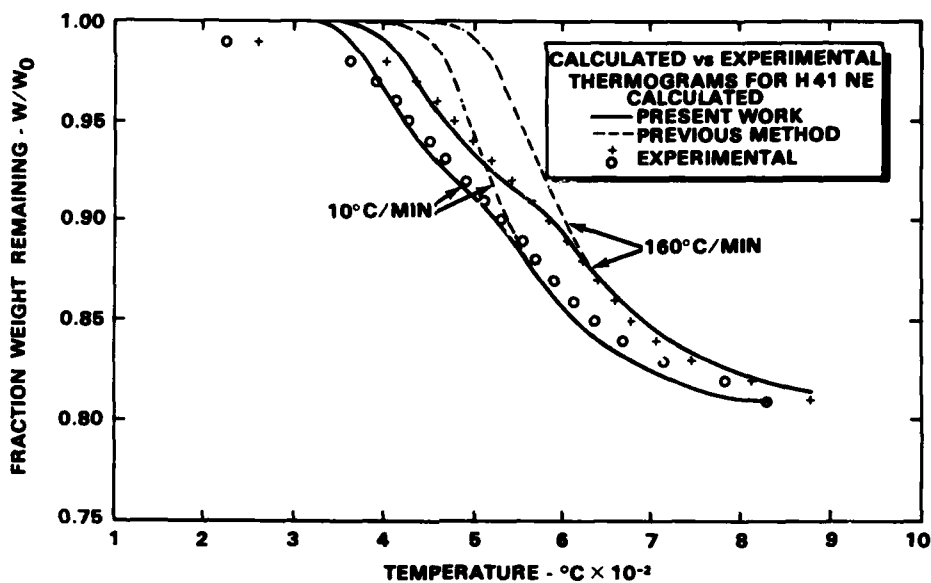


Figure 25. Comparison of Calculated Versus Experimental Weight Loss Errors for H41NE at 160°C/min and 10°C/min

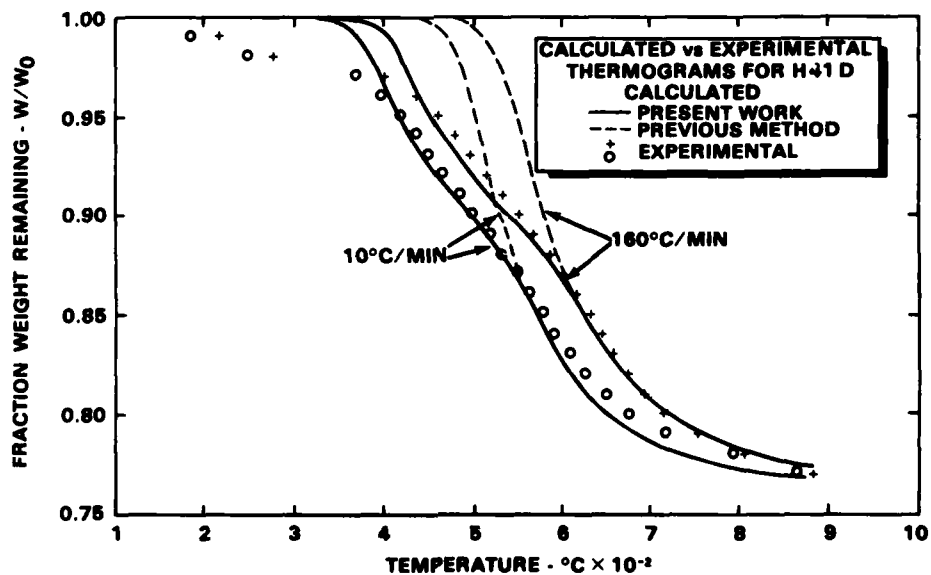


Figure 26. Comparison of Calculated Versus Experimental Weight Loss Errors for H41D at 160°C/min and 10°C/min Heating Rates

Table 3. Statistical Analysis of Errors in Computed Versus Experimental W/W_0

<u>Material</u>	<u>Average Error (%)</u>	<u>Standard Deviation (%)</u>	<u>Confidence Interval (95%)</u>
H41NE	0.33	0.58	0.22 to 0.44
H41D	0.28	0.84	0.14 to 0.42

DISCUSSION

The average activation energies calculated by the methods of Flynn and Wall and Friedman agree within 0.03 and 4.6 percent for H41NE and H41D, respectively. There was less scatter of the data using the Flynn and Wall method. This was thought to be due primarily to the errors in measuring the derivatives of the weight loss used in Friedman's method.

The kinetic parameters were calculated based on data that represented 68 percent of the total weight loss for H41D and 75 percent for H41NE. This resulted in large values of the order of reaction and pre-exponential factor for the first region. However, Friedman's results would have been similar to these had he considered the same range of decomposition.

In order to evaluate the effect of separating the reaction into two parts, the thermograms were calculated for H41NE using only the kinetic parameters for $W/W_0 \leq 0.91$. The same calculations were made for H41D for $W/W_0 \leq 0.89$. This corresponded approximately to the region of weight loss considered by Friedman. As shown by the broken lines in Figures 25 and 26, the calculated versus the experimental thermograms are in poor agreement.

By separating the reaction in this manner, the reaction order and pre-exponential factor become empirical parameters that provide a "best fit" of the data. However, this method yields an extremely accurate reproduction of the thermograms over a wide range of heating rates. This is the desired result for kinetic parameters used in thermal models.

REFERENCES

1. H. L. Friedman, "Kinetics of Thermal Degradation of Char-Forming Plastics from Thermogravimetry. Application to a Phenolic Plastic," *Journal of Polymer Science: Part C*, No. 6, pp. 183-195.

2. J. H. Flynn and L. A. Wall, "A Quick, Direct Method for the Determination of Activation Energy from Thermogravimetric Data," *Polymer Letters*, Vol. 4, (1966), pp. 323-328.
3. E. S. Freeman and B. Carroll, "The Application of Thermoanalytical Techniques to Reaction Kinetics. The Thermogravimetric Evaluation of the Kinetics of the Decomposition of Calcium Oxalate Monohydrate." *Journal of Physical Chemistry*, Vol. 62, (1958) pp. 394-397.
4. D. A. Anderson and E. S. Freeman, "The Kinetics of the Thermal Degradation of Polystyrene and Polyethylene," *Journal of Polymer Science*, Vol. 54, (1961), pp. 253-260.
5. R. W. Mickelson and I. N. Einhorn, "The Kinetics of Polymer Decomposition Through Thermogravimetric Analysis," *Thermochimica Acta*, No. 1, (1970) , pp. 147-158.
6. A. D. Baer, J. H. Hedges, J. D. Seader, K. M. Jayakar, and L. H. Wojcik, "Polymer Pyrolysis over a Wide Range of Heating Rates," *AIAA Journal*, Vol. 15, No. 10, (1977) pp. 1398-1404.
7. N. W. Burningham, and J. D. Seader "Determination of Kinetic Parameters for the Thermal Degradation of Polymers by the Quasilinearization Technique," *Thermochimica Acta*, No. 5, (1972) pp. 59-69.
8. I. J. Goldfarb, R. McGuchan, and A. C. Meeks, *Kinetic Analysis of Thermogravimetry, Part II Programmed Temperature*, AFML-TR-68-181 Part II (Wright-Patterson Air Force Base, Oh., December 1968).
9. S. D. Norem, M. J. O'Neil, and A. P. Gray, "The Use of Magnetic Transitions in Temperature Calibration and Performance Evaluation of Thermogravimetric System," *Thermochimica Acta*, No. 1, (1970), pp. 29-38.

APPENDIX
EXPERIMENTAL DATA

Experimental Data

W/W ₀	Heating Rate 160°C/min				Heating Rate 100°C/min				Heating Rate 80°C/min			
	Material				Material				Material			
	H41NE M ₀ =7.9306	H41D M ₀ =7.3061	H41NE M ₀ =7.4272	H41D M ₀ =7.8094	H41NE M ₀ =7.8858	H41D M ₀ =7.0392						
0.98	T(°C)	403.0	0.0203	390.0	0.0106	407.1	0.0190	400.0	0.0151	400.0	0.0125	
0.97	(-1/W ₀)(dW/dt) (1/min)	0.0496	0.0160	432.3	0.0312	407.1	0.0190	430.0	0.0304	430.0	0.0303	
0.96	T(°C)	460.0	0.0683	454.9	0.0436	437.7	0.0385	452.0	0.0384	431.3	0.0405	
0.95	(-1/W ₀)(dW/dt) (1/min)	0.0786	0.0682	476.5	0.0498	459.2	0.0507	472.0	0.0413	451.6	0.0465	
0.94	T(°C)	500.0	0.0827	497.1	0.0517	478.6	0.0580	492.0	0.0415	468.9	0.0497	
0.93	(-1/W ₀)(dW/dt) (1/min)	0.0815	0.0913	521.9	0.0504	495.9	0.0613	514.0	0.0393	486.2	0.0500	
0.92	T(°C)	544.0	0.0773	543.5	0.0479	513.3	0.0618	539.0	0.0378	504.5	0.0492	
0.91	(-1/W ₀)(dW/dt) (1/min)	0.0773	0.0958	565.1	0.0470	529.6	0.0608	561.0	0.0382	522.8	0.0483	
0.90	T(°C)	586.0	0.0808	586.7	0.0485	548.0	0.0607	581.0	0.0413	539.0	0.0492	
0.89	(-1/W ₀)(dW/dt) (1/min)	0.0866	0.0965	608.4	0.0533	567.4	0.0616	602.9	0.0445	557.3	0.0509	
0.88	T(°C)	623.5	0.0922	627.6	0.0571	582.7	0.0645	620.7	0.0465	573.6	0.0546	
0.87	(-1/W ₀)(dW/dt) (1/min)	0.0953	0.1063	645.8	0.0580	600.0	0.0691	639.5	0.0462	589.9	0.0581	
0.86	T(°C)	659.0	0.0934	664.0	0.0567	613.9	0.0731	659.3	0.0426	606.1	0.0607	
0.85	(-1/W ₀)(dW/dt) (1/min)	0.0831	0.1196	687.0	0.0482	627.8	0.0759	686.0	0.0332	620.2	0.0609	
0.84	T(°C)	795.2	0.0657	717.7	0.0380	640.8	0.0755	720.6	0.0259	635.4	0.0581	
0.83	(-1/W ₀)(dW/dt) (1/min)	--	0.1224	--	--	656.7	0.0718	--	--	649.5	0.0519	
0.82	T(°C)	--	0.1150	--	--	672.6	0.0639	--	--	665.7	0.0418	
0.81	(-1/W ₀)(dW/dt) (1/min)	--	0.0983	--	--	697.5	0.0501	--	--	686.9	0.0317	
0.80	T(°C)	--	0.0787	--	--	727.3	0.0379	--	--	714.2	0.0224	
0.79	(-1/W ₀)(dW/dt) (1/min)	--	0.0560	--	--	768.1	0.0250	--	--	751.6	--	

Experimental Data (Continued)

W/M ₀	Heating Rate 40°C/min				Heating Rate 20°C/min				Heating Rate 10°C/min			
	Material				Material				Material			
	H41NE M ₀ =7.6769	H41D M ₀ =7.9664	H41NE M ₀ =7.1357	H41D M ₀ =7.5368	H41NE M ₀ =7.4106	H41D M ₀ =7.6958						
	T(°C)	(-1/W ₀)(dM/dt) (1/min)	T(°C)	(-1/W ₀)(dM/dt) (1/min)	T(°C)	(-1/W ₀)(dM/dt) (1/min)	T(°C)	(-1/W ₀)(dM/dt) (1/min)	T(°C)	(-1/W ₀)(dM/dt) (1/min)	T(°C)	(-1/W ₀)(dM/dt) (1/min)
0.98	371.7	0.0051	--	--	370.6	0.0042	--	--	363.3	0.0026	--	--
0.97	412.2	0.0146	382.7	0.0060	398.6	0.0083	380.6	0.0038	392.0	0.0047	367.1	0.0019
0.96	437.1	0.0195	418.6	0.0152	423.6	0.0105	412.4	0.0086	415.6	0.0059	397.4	0.0040
0.95	456.9	0.0215	440.1	0.0210	441.2	0.0112	431.9	0.0114	430.0	0.0062	418.6	0.0057
0.94	479.7	0.0215	456.5	0.0240	460.9	0.0110	450.3	0.0127	452.5	0.0061	436.7	0.0064
0.93	495.3	0.0203	474.0	0.0254	481.7	0.0102	466.7	0.0131	469.9	0.0058	449.8	0.0065
0.92	521.2	0.0191	491.4	0.0255	504.6	0.0097	483.1	0.0130	492.5	0.0054	467.0	0.0064
0.91	542.0	0.0193	508.8	0.0250	528.4	0.0099	498.5	0.0126	514.0	0.0054	486.1	0.0062
0.90	563.8	0.0206	525.2	0.0245	548.2	0.0107	516.0	0.0123	531.4	0.0058	499.2	0.0061
0.89	584.6	0.0223	542.7	0.0246	567.9	0.0112	534.4	0.0125	556.0	0.0062	519.4	0.0062
0.88	604.1	0.0234	561.1	0.0256	587.6	0.0116	548.8	0.0131	571.4	0.0063	533.5	0.0066
0.87	621.3	0.0236	575.5	0.0274	606.9	0.0112	566.2	0.0142	591.9	0.0063	549.7	0.0071
0.86	640.5	0.0221	592.9	0.0291	627.5	0.0097	580.6	0.0149	612.8	0.0054	562.8	0.0074
0.85	665.7	0.0176	605.8	0.0303	651.1	0.0083	595.9	0.0154	635.6	0.0049	577.9	0.0075
0.84	698.1	0.0140	617.5	0.0299	685.6	0.0059	608.7	0.0150	668.2	0.0038	591.0	0.0073
0.83	--	--	634.2	0.0281	--	--	625.1	0.0138	--	--	608.4	0.0064
0.82	--	--	647.9	0.0247	--	--	638.7	0.0118	--	--	626.8	0.0053
0.81	--	--	670.4	0.0201	--	--	661.9	0.0096	--	--	649.1	0.0043
0.80	--	--	697.8	0.0154	--	--	689.0	0.0073	--	--	676.2	0.0032
0.79	--	--	732.1	0.0112	--	--	722.9	0.0052	--	--	715.9	0.0021

DISTRIBUTION

Commander
Naval Sea Systems Command
Washington, DC 20362
ATTN: SEA 62R (L. Pasiuk)
SEA 622Z (G. Montgomery)

Commander
Naval Research Laboratory
Washington, DC 20390

Chief of Naval Research
Department of the Navy
Washington, DC 20390

Chief of Naval Operations
Department of the Navy
Washington, DC 20350

Chief of Naval Material
Department of the Navy
Washington, DC 23060

Director
Defense Nuclear Agency
Washington, DC 20305

Chrysler Corporation
Department 2731
P. O. Box 29200
New Orleans, LA 70189
ATTN: R. Keefe

Martin-Marietta Aerospace
Orlando Division
P. O. Box 3837
Orlando, FL 32855
ATTN: M-P336 (T. Radovich)

Haveg Industries
Chemical Equipment Division
900 Greenbank Road
Wilmington, DE 19808
ATTN: R. Wilde

GIDEP Operation Office
Corona, CA 91720

Defense Documentation Center
Cameron Station
Alexandria, VA 22314

(12)

Library of Congress
Washington, DC 20540
ATTN: Gift and Exchange Division

(4)

Local:

E31

E41

G

G25 (Coates) (6)

G53 (Hall) (6)

N

N40

N43

N43 (Henderson) (50)

X210 (6)